

HYDROTHERMALLY SYNTHESIZED CZTS NANOPARTICLES TRANSFORMING COUNTER ELECTRODES IN DYE-SENSITIZED SOLAR CELLS

Yogesh Kumar Saini, Amanpal Singh

yogeshuor92@gmail.com, amanbakn@gmail.com

Department of Physics, University of Rajasthan, Jaipur- 302004, India

Abstract: This study introduces a cost-effective hydrothermal method for synthesizing $\text{Cu}_2\text{ZnSnS}_4$ (CZTS) nanoparticles. The synthesis process involves dissolving zinc chloride, tin(II) chloride, copper(I) chloride, and thiourea in deionized water to produce CZTS nanoparticles. The resulting nanoparticles exhibit a phase-pure kesterite structure, confirmed through Raman spectroscopy and X-ray diffraction analysis. Optical and morphological assessments revealed strong absorption in the visible range, with a band gap energy of 1.55 eV. Energy-dispersive X-ray spectroscopy (EDX) confirmed the stoichiometric composition of the nanoparticles. Used as counter electrodes (CE) in dye-sensitized solar cells (DSSCs) under AM 1.0 G light, the CZTS nanoparticles achieved a power conversion efficiency of 2.78%, compared to 3.04% for platinum CEs. These findings suggest that kesterite nanoparticles can serve as a viable, cost-effective alternative to platinum CEs in DSSCs, addressing the issue of platinum scarcity.

Introduction

CZTS, a semiconductor with a kesterite phase, has become a focal point for advancing next-generation solar devices. It is composed of

inexpensive and environmentally friendly elements such as sulfur (S), zinc (Zn), copper (Cu (I)), and tin (Sn (II)) [1, 2]. CZTS also exhibits adjustable bandgap properties (1.45-1.70 eV) and a high absorption coefficient (10^4 cm^{-1}) [3-5]. Due to these exceptional qualities, CZTS is considered a promising material for various solar cell configurations. These configurations include perovskite solar cells [6,7], quantum dot DSSCs [8, 9], thin-film solar cells [10-12], and dye-sensitized solar cells (DSSCs) [13-15].

Dye-sensitized solar cells, or DSSCs, have generated a lot of interest because of their inexpensive manufacturing costs. One of the most crucial parts of DSSCs are the counter electrodes (CEs), which catalyze the redox electrolyte's reduction and gather free electrons generated by photolysis from the external circuit. [14]. The primary use of platinum (Pt) in dye-sensitized solar cells (DSSCs) is as the counter electrode (CE). It is applied on a glass substrate that has been coated in fluorine-doped tin oxide (FTO) [15]. However, efforts are being made to replace platinum (Pt) in DSSCs due to its high cost and limited availability. [16]. As substitutes for platinum for the counter electrode in DSSCs, researchers are looking into conjugated polymer-based materials [16,17],

carbon-based materials [18, 19], cobalt sulphide/selenide [20,21], kesterite thin films and nanoparticles [22-29], and a variety of other inorganic materials [30-34]. CZTS nanoparticles (NPs) have shown significant potential as catalytic materials in DSSCs. The performance of CZTS-based DSSCs is significantly influenced by the synthesis method, elemental compositions, and morphology of CZTS CEs [14, 15]. An efficiency of 5.65% was demonstrated by a CZTS CE that was produced using a solvothermal technique on an FTO (fluorine-doped tin oxide, SnO₂: F) substrate [35]. Wurtzite and kesterite phase CZTS nanocrystalline thin films were used as CEs by Kong et al. [17], with wurtzite CZTS demonstrating a higher efficiency (6.23%) than kesterite phase CZTS CE (4.89%). The best reported efficiency for CZTS-based counter electrodes to date, 8.67%, was achieved by Chen et al. [36] using nanoleaf-like plates of CZTS CEs created by solvothermal treatment on electrodeposited Cu₂ZnSnS₄ films in dye-sensitized solar cells.

In this paper, the role of CZTS NP fabricated by hydrothermal route as counter electrode (CE) in DSSCs is investigated. The synthesized CZTS NPs show a good catalytic behaviour when used as the CE in DSSCs.

Experimental methods Deposition of TiO₂ nanorods as a working electrode

The TiO₂ photoanode was air-annealed at 450°C for 30 minutes and then cooled to 80°C.

Subsequently, the annealed photoanodes were immersed in 0.5 mM ethanolic solutions of N719 dye (Dyesol) for 24 hours [37].

Deposition of CZTS NPs layers as a counter electrode

A hydrothermal approach was used to create CZTS NPs using 0.0125 M zinc chloride, 0.02 M cuprous chloride, 0.01 M stannous chloride, and 0.15 M thiourea as precursors that have been dissolved in deionized water. After 30 min of vigorous stirring, the resultant mixture was poured into a 75% capacity Teflon-lined stainless-steel autoclave. For twenty-four hours, the autoclave was kept at 230°C in a hot air oven. The oven was then let to naturally cool to room temperature. The product with a black hue was gathered, repeatedly cleaned using ethanol and distilled water, and then dried for ten hours at 80°C. To create the counter electrode (CE), ethanol was used to scatter CZTS NPs, which were then spin-coated onto a glass substrate coated with FTO (7 Ωsq⁻¹, Pilkington). Annealing for one minute at 200°C in the air came next. A Pt counter electrode (CE) was made by drop-casting a few drops of H₂PtCl₆ solution (2 mgmL⁻¹ in ethanol) onto FTO glass (7 Ωsq⁻¹, Pilkington), then annealing it for 15 minutes at 410°C [37].

Fabrication of DSSC

In order to assemble the DSSC, the photoanode and counter electrode were sandwiched together

and sealed with a 25 μm thick layer of surlyn (Solaronix SA), which also functioned as a spacer. A pre-drilled hole in the counter electrode was used to inject the electrolyte, which was 0.6 M 1,3-dimethylimidazolium iodide, 0.1 M lithium iodide, 0.05 M iodine, 0.5 M 4-tert-butylpyridine (TBP), and 0.6 M benzylmethylimidazolium iodide in acetonitrile: valeronitrile (85:15). After injecting the electrolyte, the hole was sealed with surlyn and a cover glass slide. To define the area of the solar cell, a mask with a 0.23 cm^2 area was placed on the photoelectrode [37].

Characterizations

Cu $K\alpha$ line $\lambda = 1.5405 \text{ \AA}$ was employed in an X-ray diffractometer (Rigaku) to study the crystal structure of CZTS NPs. Using the JSM-7610F plus, the surface morphology and elemental content (FESEM and EDX) of the NP were assessed. Utilizing a Shimadzu UV- 2600 spectrophotometer, the optical characteristics of CZTS NPs were measured. I-V measurements were performed in 1.0 SUN was performed by Solar simulator SSX-50 from Enil Technology Co. Ltd.

Results and discussion:

CZTS samples crystal structures and phases were evaluated using X-ray diffraction (XRD) techniques. Moreover, it was clear that the synthesized CZTS NPs showed different peaks at $2\theta = 28.7, 47.6,$ and 56.3° corresponded to the

crystal planes (112), (220), and (312) respectively, which were suggestive of a kesterite structure (space group: $I42m$) with lattice parameters of $a = b = 5.427 \text{ \AA}$ and $c = 10.848 \text{ \AA}$. This observation is in good agreement with the stated data on lattice parameters [37, 38]. No additional peaks that would have been predicted for binary compounds like CuS, ZnS, and SnS, or ternary compounds like Cu_2SnS_3 , were found.

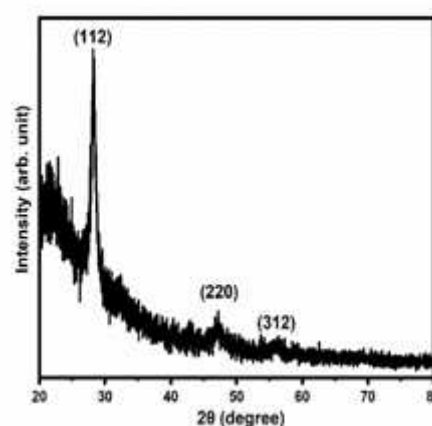


Figure 1. Powder XRD patterns of the hydrothermally-synthesized CZTS NPs

FESEM (Field Emission Scanning Electron Microscopy) was used to examine the morphology of the synthesized CZTS NPs particles. Figure 2a, respectively, shows SEM micrographs and EDX spectra of the as-synthesised CZTS NPs. The pictures show that the particle size of CZTS nanoparticles (NPs) is in the nanometre range. Agglomerations are readily visible in the SEM pictures of the NPs [37]. The elemental composition determined by EDX spectra are shown in Figure 2b.

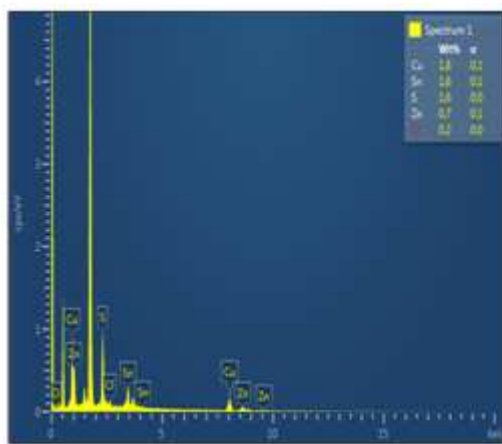
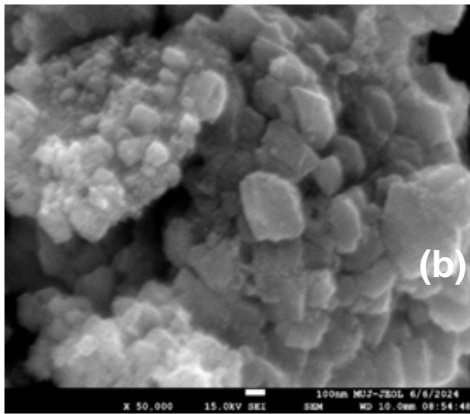


Figure 2. FESEM image and corresponding EDX spectra of CZTS NPs

The optical properties such as reflectance and band gap of CZTS NPs powder were investigated in the wavelength range 350 – 800 nm using UV-Visible spectroscopy. The reflectance spectra of CZTS NPs are shown in figure 3 (a). The optical direct bandgap energy (E_g) of CZTS NPs powder is evaluated from reflectance spectrum using Kubelka–Munk function, $F(R_\infty)$:

$$F(R_\infty)hv = (hv - E_g)^{1/2}$$

where $F(R_\infty)$ is Kubelka–Munk function, h is Planck's constant, ν wave number.

$F(R_\infty)$ is calculated from reflectance spectra:

$$F(R_\infty) = \frac{(1 - R_\infty)^2}{2R_\infty}$$

where

$$R_\infty = R(\%)/R_{ref}(\%),$$

R_{ref} : reflectance of reference sample ($BaSO_4$).

The bandgap energy (E_g) of CZTS NPs is estimated by extrapolating a tangent on linear part of $(F(R_\infty)hv)^2$ versus (hv) plot to meet the hv axis as shown in figure 3(b). The bandgap of CZTS is found to be 1.55 eV [37, 39].

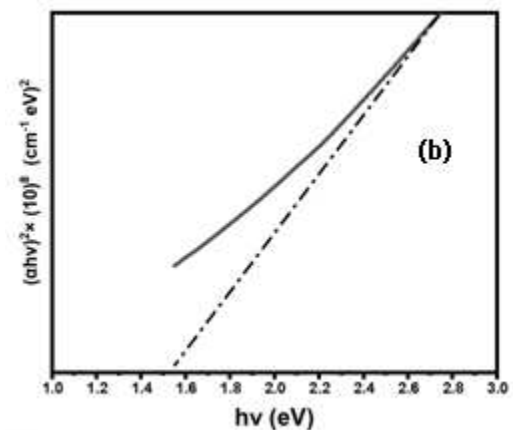
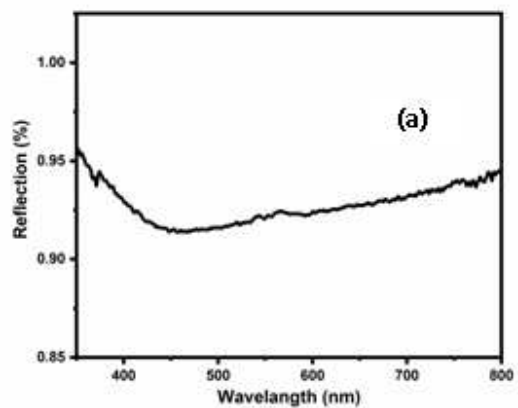


Figure 3. (a) UV-Vis reflection spectra (b) Optical band gaps of CZTS powder.

CZTS and Pt CEs photovoltaic performance in DSSCs

The DSSC employing the CZTS counter electrode (CE) demonstrates notable

photovoltaic capabilities. It achieves an overall power conversion efficiency (PCE) of 2.78%, with an open-circuit voltage (V_{OC}) of 0.616 V and a short-circuit current density (J_{SC}) of 7.92 mAcm^{-2} (Table 1). The improved V_{OC} in the CZTS-based DSSC, compared to the Pt CE, can be attributed to lower charge transfer resistance (RCT) and higher cathodic current density [37]. In comparison, the DSSC with the platinum (Pt) CE shows a slightly higher efficiency of 3.04%. Although the efficiency of the DSSC with the CZTS CE is lower than that with the Pt CE, it is significant considering that CZTS is a cost-effective, earth-abundant, and easily synthesized material. The measured lower efficiency of the fabricated DSSCs can also be attributed to the low concentration of dye used during the measurements [20]. This demonstrates that with further optimization, CZTS can serve as a viable alternative to platinum for counter electrodes in dye-sensitized solar cells.

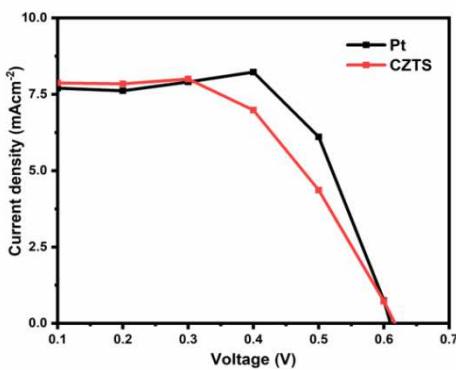


Figure 4. Photovoltaic performance of DSSCs with Pt and CZTS counter electrode

Counter electrode	Pt	CZTS
J_{SC} (mAcm^{-2})	7.77	7.92
V_{OC} (V)	0.610	0.616
FF (%)	64.37	57.21
PCE (%)	3.04	2.78

Conclusions

Kesterite CZTS nanoparticles were hydrothermally synthesized using an aqueous solution of zinc chloride, cuprous chloride, stannous chloride, and thiourea. These CZTS nanoparticles exhibit a bandgap of 1.55 eV. The synthesized CZTS nanoparticle layer was spin-coated onto an FTO-coated glass substrate and subsequently used as the counter electrode (CE) in dye-sensitized solar cells (DSSCs). The CZTS CE demonstrated catalytic performance with an efficiency of 2.78%, comparable to the standard platinum electrode. Additionally, the V_{OC} value using the CZTS counter electrode was found to be higher than that of the Pt CE. This hydrothermal synthesis method, utilizing inexpensive, non-toxic, and readily available materials, presents a viable alternative to platinum for counter electrodes in DSSCs.

Acknowledgment: The authors would like to extend their gratitude to the DST SERB for supporting this work through grant ECR/2017/003055.

References

1. B. D. Mitzi, O. Gunwan, T. K. Tordov, K. Wang, S. Ghuha, The path towards a high-performance solution-processed kesterite solar cell. *Sol Energy Mater Sol Cells* 95:1421–1436, 2011.
2. H. Karagiri, K. Jimbo, S. Yamada, T. Kamimura, S. W. Maw, T. Fukano, T. Ito, Enhanced conversion efficiency of $\text{Cu}_2\text{ZnSnS}_4$ – based thin film solar cells by using preferential etching technique. *Appl Phys Express* 1:041201, 2008.
3. T. Kameyama, T. Osaki, K. Okazaki, T. Shibayama, A. Kudo, S. Kuwabata, T. Torimo, Preparation and photoelectrochemical properties of densely immobilized $\text{Cu}_2\text{ZnSnS}_4$ thin films. *J Mater Chem* 20:5319–5324, 2010.
4. K. Ito, T. Nakazawa, Electrical, and optical properties of stannite type quaternary semiconductor thin films. *J Appl Phys* 27:2094–2097, 1988.
5. H. Katagiri, CuZnSnS thin films solar cells, *Thin Solid Films* 480-481:426–432, 2005.
6. S. B. Patel, A. H. Patel, J. V. Gohel, A novel and cost effective CZTS transport material applied in perovskite solar cells. *J Mater Sci Mater Electron* 20:7677–7687, 2018.
7. S. B. Patel, V. H. Gohel, Synthesis of novel counter electrode by combination of mesoporous- microporous CZTS films for enhanced performance of quantum dot sensitized solar cells. *J Mater Sci Mater Electron* 0:1–8, 2018.
8. B. Bai, D. Kou, W. Zho, S. Wu, Applications of quaternary $\text{Cu}_2\text{ZnSnS}_4$ quantum dot sensitized solar cells based on hydrolysis approach. *Green Chem* 17:4377–4382, 2015.
9. S. C. Riha, B. A. Parkinson, A. L. Prieto, compositionally tunable $\text{Cu}_2\text{ZnSnS}_x\text{Se}_{4-x}$ nanocrystals: probing the effect of Se inclusion in mixed chalcogenide thin films. *J Am Chem Soc* 133:15272.
10. T. K. Tordov, J. Tang, S. Bag, O. Gunwan, T. Gokmen, Y. Zhu, B. D. Mitzi, Beyond 11% efficiency: characteristics of state of the art $\text{Cu}_2\text{ZnSn}(\text{S},\text{Se})$ solar cells. *Adv Energy Mater* 3:34–38, 2011.
11. M. A. Green, Y. Hishikawa, E. D. Dunlop, D. H. Levi, J. H. Ebinger, Solar cell efficiency table (version 51). *Prog Photovolt* 26:3–12, 2018.
12. W. Wang, M. T. Winkler, O. Gunwan, T. Gokman, T. K. Tordov, Y. Zhu, B. D. Mitzi, Device characteristics of CZTSSe thin film solar cells with 12.6%

- efficiency. *Adv Energy Mater* 4:1301465, 2014.
13. H. Chen, D. Kou, Z. Chang, W. Zhou, Z. Zhou, S. Wu, Effect of crystallisation of $\text{Cu}_2\text{ZnSnS}_x\text{Se}_{4-x}$ counter electrode on the performance of for efficient dye sensitized solar cells. *ACS Appl Mater Interface* 6:20664, 2014.
 14. S. L. Chen, A. C. Xu, J. Tao, H. J. Tao, Y. Z. Shen, L. M. Zhu, In situ synthesis of two-dimensional leaflike plate arrays as Pt- free counter electrode for efficient dye sensitized solar cell. *Green Chem* 18(9):2793–280, 2016.
 15. S. S. Mali, P. S. Patil, C. K. Hong, Low cost electrospun crystalline kesterite $\text{Cu}_2\text{ZnSnS}_4$ nanofibre counter electrodes for efficient dye sensitized solar cells. *ACS Appl Mater Interface* 6:1688, 2014.
 16. H.N. Tsao, J. Burschka, C. Yi, F. Kessler, M.K. Nazeeruddin, M. Gratzel, *Energy* ∞ *Environ. Sci.* 4, 4921, 2011.
 17. Y. Saito, T. Kitamura, Y. Wada, S. Yanagida, *Chem. Lett.* 31, 1060, 2002.
 18. S.G. Hashmi, J. Halme, T. Saukkonen, E.L. Rautama, P. Lund, *Chem. Chem. Phys.* 15, 17689, 2013.
 19. Y. Xiao, J.Y. Lin, J. Wu, S.Y. Tai, G. Yue, T.W. Lin, *J. Power Sources* 233,320, 2013.
 20. S.K. Swami, N. Chaturvedi, A. Kumar, R. Kapoor, V. Dutta, J. Frey, T. Moehl, M. Gratzel, S. Mathew, M.K. Nazeeruddin, *J. Power Sources* 275, 80, 2015 .
 21. Y. Zhao, J. Duan, Y. Duan, H. Yuan, Q. Tang, *Mater. Lett.* 218, 76, 2018.
 22. S.K. Swami, N. Chaturvedi, A. Kumar, V. Dutta, *Electrochim. Acta* 263, 26, 2018.
 23. Y. Du, J. Fan, W. Zhou, Z. Zhou, J. Jiao, S. Wu, *ACS Appl. Mater. Interfaces* 4, 1796, 2012.
 24. Y. Xie, C. Zhang, F. Yue, Y. Zhang, Y. Shi, T. Ma, *RSC Adv.* 3, 23264, 2013.
 25. Y. Xie, C. Zhang, G. Yang, J. Yang, X. Zhou, J. Ma, *J. Alloy. Comp.* 696, 938, 2017.
 26. S. Wozny, K. Wang, W. Zhou, *J. Mater. Chem. A* 1,15517, 2013.
 27. L. Bai, J.N. Ding, N.Y. Yuan, H.W. Hu, Y. Li, X. Fang, *Mater. Lett.* 112, 219, 2013.
 28. X. Wang, W.H. Zhou, Z.J. Zhou, Z.L. Hou, J. Guo, S.X. Wu, *Electrochim. Acta* 104, 26, 2013.
 29. S.S. Mali, P.S. Patil, C.K. Hong, *ACS Appl. Mater. Interfaces* 6, 1688, 2014.
 30. J. Wang, Q. Tang, B. He, P. Yang, *J. Power Sources* 328, 185, 2016.
 31. P. Yang, C. Mab, Q. Tang, *Electrochim. Acta* 184, 226, 2015.
 32. J. Duan, Q. Tang, H. Zhang, Y. Meng, L.Yu, P. Yang, *J. Power Sources* 302,361, 2016.
 33. W. Hou, Xiao, G. Han, *Angew. Chem.* 129, 9274, 2017.

34. Z. Pang, Y. Zhao, Y. Duan, J. Duan, Q. Tang, L. Yu, J. Energy Chem 000, 2018.
35. S. Chen, H. Tao, Y. She, L. Zhu, X. Zeng, J. Tao, T. Wang, Facile synthesis of single crystalline sub-micron $\text{Cu}_2\text{ZnSnS}_4$ (CZTS) powders using solvothermal treatment. RSC Adv 5:6682, 2015.
36. J. Kong, Z. J. Zhu, M. Li, W. H. Zhou, S. J. Yuan, R. Y. Yao, Y. Zho, S. X. Wu, Wurtzite copper zinc tin sulphide as a superior counter electrode material for dye sensitized solar cell. Nanoscale Res Lett 8(1):464, 2013.
37. S.K. Swami, N. Chaturvedi, A. Kumar, N. Chander, V. Dutta, D.K. Kumar, A. Ivaturi, S. Senthilarasu, H.M. Upadhyaya, Effect of zinc precursor on $\text{Cu}_2\text{ZnSnS}_4$ nanoparticles synthesized by the solvothermal method and its application in dye-sensitized solar cells as the counter electrode, Phys. Chem. Chem. Phys. 16, 23993, 2014.
38. H. Ju Chen et al Structural and photoelectron spectroscopic studies of band alignment at the $\text{Cu}_2\text{ZnSnS}_4/\text{CdS}$ heterojunction with slight Ni doping in $\text{Cu}_2\text{ZnSnS}_4$, J. Phys. D: Appl. Phys. 49 335102, 2016.
39. S. M. Camara et al Easy hydrothermal preparation of $\text{Cu}_2\text{ZnSnS}_4$ (CZTS) nanoparticles for solar cell application, Nanotechnology 24 495401, 2013.